elements will belong to G_1 after a few iterations and consequently, the beam will be fully stressed, so that both cases distinguished in Sec. 2 may be computed by the same technique. Figure 2 gives the optimal design for various values of $\hat{\sigma}$.

References

[1] Barnett, R. L., "Minimum Weight Design of Beams for Deflection," *Proceedings of the ASCE*, Vol. 87, No. EM1, 1961, pp. 75–109.

[2] Huang, N. C. and Tang, H. T., "Minimum Weight Design of Elastic Sandwich Beams with Deflection Constraints," *Journal of Optimization Theory and Applications*, Vol. 4, No. 4, Oct. 1969, pp. 277–298.

[3] Chern, J. M. and Prager, W., "Minimum-Weight Design of Statically Determinate Truses Subject to Multiple Constraints," *International Journal for Solids and Structures*, to be published.

[4] Kuhn, H. W. and Tucker, A. W., "Nonlinear Programming," *Proceedings of the 2nd Berkeley Symposium on Mathematics, Statistics and Probability*, University of California Press, 1950, Berkeley, Calif., pp. 481–492.

[5] Shield, R. T. and Prager, W., "Optimal Design for Given Deflection," *Journal of Applied Mathematics and Physics*, Vol. 21, 1970, pp. 513–523.

A Specialization of Jones' Generalization of the Direct-Stiffness Method of Structural Analysis

SAMUEL W. KEY*

Sandia Laboratories, Albuquerque, N. Mex.

JONES[1] has presented a variational formulation which accounts for displacement discontinuities across element boundaries. The purpose of this Note is to present a specialized version of his results. For classical elasticity, Jones considered the functional

$$\pi(u_i,\alpha^i,\beta^i) = \int_V (\tfrac{1}{2}C^{ijrs}u_{i,j}u_{r,s} - f^iu_i)dv - \int_{S_{E\bar{T}}} \bar{T}^iu_ids - \int_{S_{E\bar{U}}} \alpha^i(u_i - \bar{u}_i)ds - \int_{S_I} \beta^i(u_i^1 - u_i^2)ds - \int_{S_I} \bar{T}^i\tfrac{1}{2}(u_i^1 + u_i^2)ds$$

where u_i = the covariant components of the displacement vector; $\alpha^i\beta^i$ = Lagrange multipliers; C^{ijrs} = the contravariant components of the elasticity tensor; f^i = the contravariant components of the body force vector; T^i = the contravariant components of the surface traction vector; V = the volume of the body; S_E = the exterior surface of the body; S_I = an interior surface in the body; $S_{E\bar{T}}$ = that portion of the exterior surface where a traction $\bar{T}^i$ is prescribed; $S_{E\bar{U}}$ = that portion of the exterior surface where a displacement u_i is prescribed.

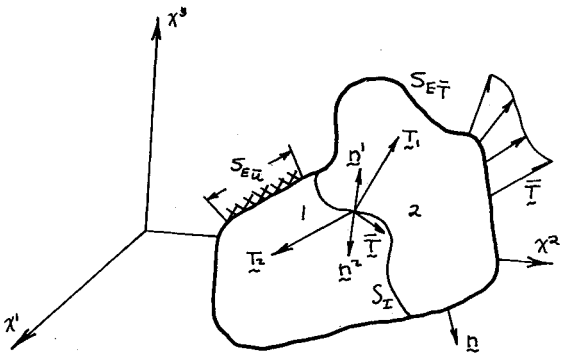

Fig. 1 Body with an interior surface.

The superscripts and subscripts 1 and 2 in the interior surface integrals denote quantities on either side of the surface. The commas denote covariant derivatives. Figure 1 depicts a body with an interior surface.

Taking the variation of π results in

$$\delta\pi = \int_V (C^{ijrs}u_{r,s}\delta u_{i,j} - f^i\delta u_i)dv - \int_{S_{E\bar{T}}} \bar{T}^i\delta u_ids - \int_{S_{E\bar{U}}} \alpha^i\delta u_ids - \int_{S_{E\bar{U}}} (u_i - \bar{u}_i)\delta\alpha^ids - \int_{S_I} \beta^i\delta(u_i^1 - u_i^2)ds - \int_{S_I} (u_i^1 - u_i^2)\delta\beta^ids - \int_{S_I} \bar{T}^i\tfrac{1}{2}\delta(u_i^1 + u_i^2)ds$$

Applying the divergence theorem results in

$$\delta\pi = -\int_V [(C^{ijrs}u_{r,s})_{,j} + f^i]\delta u_idv + \int_{S_{E\bar{T}}}(T^i - \bar{T}^i)\delta u_ids + \int_{S_{E\bar{T}}} (T^i - \alpha^i)\delta u_ids - \int_{S_{E\bar{U}}} (u_i - \bar{u}_i)\delta\alpha^ids + \int_{S_I} \tfrac{1}{2}(T_1^i + T_2^i - \bar{T}^i)\delta(u_i^1 + u_i^2)ds - \int_{S_I} (u_i^1 - u_i^2) \times \delta\beta^ids - \int_{S_I} [\beta_i - (T_1^i - T_2^i)/2]\,\delta(u_i^1 - u_i^2)ds$$

where $T^i = C^{ijrs}u_{r,s}n_j$. This result can be specialized in the following way. The α^i and β^i are selected as $\alpha^i = T^i = C^{ijrs}u_{r,s}n_j$ on $S_{E\bar{U}}$, $\beta^i = \frac{1}{2}(T_1^i - T_2^i) = \frac{1}{2}(C^{ijrs}u_{r,s}{}^1n_j{}^1 - C^{ijrs}u_{r,s}{}^2n_j{}^2)$ on S_I. Making these substitutions in the functional π results in a new functional Γ:

$$\Gamma(u_i) = \int_V (\tfrac{1}{2}C^{ijrs}u_{i,j}u_{r,s} - f^iu_i)dv - \int_{S_{E\bar{T}}} \bar{T}^iu_ids - \int_{S_{E\bar{U}}} T^i(u_i - \bar{u}_i)ds - \int_{S_I} \tfrac{1}{2}(T_1^i - T_2^i)(u_i^1 - u_i^2)ds - \int_{S_I} \bar{T}^i\tfrac{1}{2}(u_i^1 + u_i^2)ds$$

Taking the variation results in

$$\delta\Gamma = \int_V (C^{ijrs}u_{r,j}\delta u_{i,s} - f^i\delta u_i)dv - \int_{S_{E\bar{T}}} \bar{T}^i\delta u_ids - \int_{S_{E\bar{U}}} (u_i - \bar{u}_i)\delta T^ids - \int_{S_{E\bar{U}}} T^i\delta u_ids - \int_{S_I} \tfrac{1}{2}(u_i^1 - u_i^2)\delta(T_1^i - T_2^i)ds - \int_{S_I} \tfrac{1}{2}(T_1^i - T_2^i) \times \delta(u_i^1 - u_i^2)ds - \int_{S_I} \bar{T}^i\tfrac{1}{2}\delta(u_i^1 + u_i^2)ds$$

Using the divergence theorem results in

$$\delta\Gamma = -\int_V [(C^{ijrs}u_{r,s})_{,j} + f^i]\delta u_idv + \int_{S_{E\bar{T}}} (C^{ijrs}u_{r,s}n_j - \bar{T}^i)\delta u_ids - \int_{S_{E\bar{U}}} (u_i - \bar{u}_i)\delta T^ids - \int_{S_I} \tfrac{1}{2}(u_i^1 - u_i^2) \times \delta(T_1^i - T_2^i)ds + \int_{S_I} \tfrac{1}{2}(T_1^i + T_2^i - \bar{T}^i)\delta(u_i^1 + u_i^2)ds$$

Thus, if an arbitrary choice of displacements is made

$$u_i = \sum_{\alpha=1}^{n} a_{i\alpha}g_\alpha(x^i)$$

then extremizing Γ for this choice results in the approximate satisfaction of equilibrium in the interior, $(C^{ijrs}u_{r,s})_{,j} + f^i = 0$, stress jump, surface load equilibrium on the interior surfaces, $T_1^i + T_2^i - \bar{T}^i = 0$, the static or stress boundary conditions, $T^i = \bar{T}^i$, the displacement boundary conditions, $u^i = \bar{u}^i$, and the displacement discontinuities on the interior surfaces, $u_i{}^1 - u_i{}^2 = 0$. Thus, in the Direct-Stiffness method, element displacements selected for use with this functional need not be "compatible" along element boundaries. The new functional Γ does not require an independent assumption on the behavior of the Lagrange multipliers α_i and β_i found in the functional π. In essence, the field equations of the functional π involving the Lagrange multipliers have been satisfied exactly. The functionals π and Γ correspond to the functionals M and N, respectively, discussed by Prager.[2]

Received January 11, 1971. This work was supported by the U.S. Atomic Energy Commission.

* Staff Member.

References

[1] Jones, R. E., "A Generalization of the Direct-Stiffness Method of Structural Analysis," *AIAA Journal*, Vol. 2, No. 5, May 1964.

[2] Prager, W., "Variational Principles for Linear Elastostatics for Discontinuous Displacements, Strains and Stresses," *Recent Progress in Applied Mechanics: The F. Odqvist Volume*, Wiley, New York, 1967, pp. 463–474.

Shock Interaction Effect on a Flapped Delta Wing at $M = 8.2$

DHANVADA MADHAVA RAO*
NASA Langley Research Center, Hampton, Va.

THE effects of wave interactions on hypersonic vehicles have received considerable attention in recent years. Edney[1] has identified different types of interactions, and some examples of such interactions in practical situations have recently been reviewed by Korkegi.[2] Although the emphasis has been on local surface heating problems associated with wave-interaction fields, in some instances the modification of surface pressure distributions causes significant variations in vehicle aerodynamic characteristics. The loss in stability of flare-stabilized missiles caused by the interaction of bow and flare shocks[3] is an example. An analogous situation was observed in a recent investigation of trailing-edge flap effectiveness on delta wings at hypersonic speeds.[4] Balance measurements on a 76° swept delta wing with a 30° positively deflected full-span flap (conducted in the Imperial College Gun Tunnel fitted with a $M = 8.2$ contoured nozzle) yielded aerodynamic coefficients significantly below inviscid estimates. Flow visualization results suggested that the loss in aerodynamic loading was more than could reasonably be adduced to separation effects. From pressure measurements and oil flow studies, a considerable proportion of the flap appeared to be influenced by the reflected wave emanating from the intersection of the wing and flap shocks. This phenomenon has been discussed in the literature[5] and is well evident in the experimental flap pressure distributions on the two-dimensional model analyzed by Hill.[6]

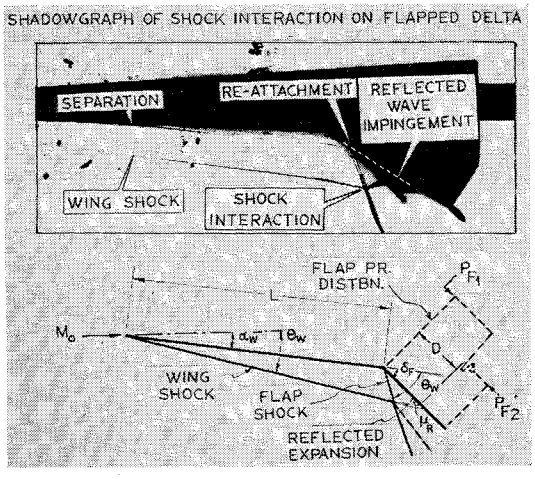

Fig. 1 Wing shock/flap shock interaction.

Received December 4, 1970. This work was performed at the Aeronautics Department, Imperial College, London, under a research contract awarded by the British Ministry of Technology.

* Research Associate, Hypersonic Vehicles Division. Member AIAA.

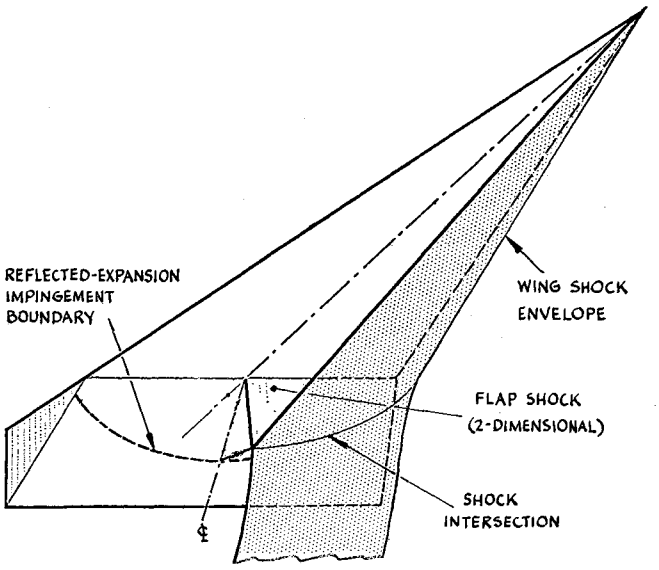

Fig. 2 Model of shock interaction on flapped delta wing.

In this Note, a simple method to estimate the reflected wave impingement effect on the aerodynamic characteristics of a flappaed delta wing, using a simple flow model, is presented. Experimental measurements[4] have been used to assess the proposed prediction method.

The shadowgraph presented in Fig. 1 serves to illustrate the phenomenon under consideration. As depicted in the sketch, the intersection of the wing and flap shocks in an inviscid hypersonic flow generates a merged shock, a slip layer and a reflected wave. At hypersonic Mach numbers and with the deflection angles of interest, the reflected wave is an expansion, and this is the case considered here. A fall in pressure occurs on the flap surface at the impingement position of the reflected expansion, the pressure asymptotically approaching the far downstream value assumed to correspond to a single shock deflection of the freestream through the combined angle $\alpha_w + \delta_F$ via further wave reflections. The solutions presented in Ref. 5 indicate that the approach to the final pressure is quite rapid downstream of the first impingement, as also found experimentally.[6]

The distance from the flap hinge line to the first reflected expansion is given by

$$\frac{D}{L} = \frac{\cot(\theta_F - \delta_F) + \cot\mu_R}{\cot(\theta_w - \alpha_w) - \cot\theta_F} \cdot \frac{\sin(\theta_F - \delta_F)}{\sin\theta_F} \qquad (1)$$

(see Fig. 1).

The three-dimensional shock interaction on a flapped delta in inviscid hypersonic flow is depicted in Fig. 2. The wing shock envelope is calculated from delta wing solutions, viz., Babaev[7] for attached leading-edge shock and Squire[8] for both attached and detached shocks. With an unswept hinge-line, the flap shock may be reasonably assumed to be locally two-dimensional up to the interaction. With attached wing shock, the local Mach number upstream of the flap shock is obtained from oblique shock theory, whereas in the case of detached shock, conical shock solution may be used as a reasonable approximation. Application of Eq. (1) along conical rays then yields the reflected expansion impingement boundary in the plane of the flap.

The calculated boundaries are compared with some experimental observations based on pressure measurements and oil flow visualization in Fig. 3 at varying incidence angle. The expansion impingement boundary may be approximately located by the isobar which terminates the plateau region and marks the beginning of pressure fall (Fig. 3a). The oil flow (Fig. 3b) provides a direct visualization of the reflected-expansion footprint as a curved band across the oil streaks.